# THE EFFECT OF ISOMERIC ISOPRENE EPOXYDIOL STRUCTURES ON THE SULFUR MASS BALANCE IN FINE PARTICULATE MATTER

Caitlin Anne Rose

A thesis submitted to the faculty at the University of North Carolina at Chapel Hill in partial fulfillment of the requirements for the degree of Master of Science in the Department of Environmental Science and Engineering in the Gillings School of Global Public Health.

Chapel Hill
2019

Approved by:

Jason D. Surratt

Barbara Turpin

Avram Gold

## ABSTRACT

Caitlin Anne Rose: The Effect of Isomeric Isoprene Epoxydiol Structures on the Sulfur Mass Balance in Fine Particulate Matter
(Under the direction of Jason D. Surratt)

Atmospheric fine particulate matter ($PM_{2.5}$) is critical to climate, air quality, and human health. Recently, acid-driven multiphase chemistry of isoprene-derived epoxydiols (IEPOX) has been demonstrated to substantially yield $PM_{2.5}$ through organosulfate (OS) formation; however, its role on the modification and fate of inorganic sulfate aerosol remains uncertain. This study assessed the effect of isomeric IEPOX structures (*trans-β*-IEPOX versus *δ*-IEPOX) on sulfate aerosol reactivity and product distribution at varying IEPOX-to-sulfate (IEPOX:$SO_4^{2-}$) ratios. Under all ratios examined, *trans-β*-IEPOX converted more sulfate into organic forms, and higher sulfate mass closures than δ-IEPOX were obtained. At higher IEPOX:$SO_4^{2-}$ ratios, *δ*-IEPOX-derived OS monomers overtook the total OS mass, possibly due to OS hydrolysis to inorganic sulfate during sample storage. Future work should examine the roles of sample storage, aerosol viscosity, phase state and acidity on these reported effects. Moreover, alternative analytical methods and authentic oligomeric OS standards are urgently needed to quantify missing OS mass.

## ACKNOWLEDGEMENTS

I would like to thank the members of my committee, Jason D. Surratt, PhD, Barbara Turpin, PhD, and Avram Gold, PhD; without your support and guidance, this work would not have come to fruition. I would also like to thank the members of the Surratt and Turpin laboratories for your encouragement and advice through this process. Finally, I would like to thank the Department of Environmental Science and Engineering for generously providing the funding I needed to pursue my graduate degree.

## TABLE OF CONTENTS

## LIST OF TABLES

## LIST OF FIGURES

## LIST OF ABBREVIATIONS

| | |
|---|---|
| AAS | Acidified Ammonium Sulfate |
| ACSM | Aerosol Chain Speciation Monitor |
| BVOC | Biogenic volatile organic compound |
| CIMS | Chemical Ionization Mass Spectrometer |
| DMA | Differential Mobility Analyzer |
| GC/EI-MS | Gas chromatography/electron ionization mass spectrometry |
| HILIC | Hydrophilic Interaction Liquid Chromatography |
| IC | Ion Chromatography |
| IEPOX | Isoprene Expoxydiol |
| ISOPOOH | Isoprene hydroxyhydroperoxides |
| LC/ESI-MS | Liquid chromatography interfaced to electrospray ionization mass spectrometry |
| $NO_x$ | Nitrogen oxides ($NO + NO_2$) |
| $NO_3$ | Nitrate radical |
| OA | Organic aerosol |
| OH | Hydroxyl radical |
| OM | Organic matter |
| OS | Organosulfates |
| $O_3$ | Ozone |
| PILS | Particle into Liquid Sampler |
| PM | Particulate Matter |
| $PM_{2.5}$ | Fine Particulate Matter |
| POA | Primary Organic Aerosol |
| PPB | Parts Per Billion (Mixing Ratio) |
| $RO_2$ | Peroxy radical |
| RH | Relative humidity |
| RPLC | Reverse Phase Liquid Chromatography |

| | |
|---|---|
| SEMS | Scanning Electrical Mobility Scanner |
| SOA | Secondary Organic Aerosol |
| SOAS | Southern Oxidant and Aerosol Study |
| UPLC/ESI-HR-QTOFMS | Ultra performance liquid chromatography/electrospray ionization high-resolution quadrupole time-of-flight mass spectrometry |
| US | United States |
| VOC | Volatile Organic Compound |

# CHAPTER I: INTRODUCTION

An aerosol is defined as a suspension of liquid or solid particles in a gaseous medium. Atmospheric fine particulate matter ($PM_{2.5}$), which is defined as aerosol particles with aerodynamic diameters $\leq 2.5$ μm, has many implications for atmospheric chemical processes, air quality, visibility, and human health. Due to the ability to reflect and scatter incoming solar radiation, as well as their ability to act as cloud condensation nuclei, aerosols can contribute to a local cooling effect.[1] This local scale cooling, though uncertain, has important implications for regional-scale climates.[2] Additionally, inhalation of atmospheric $PM_{2.5}$ has been linked to potential human health risks; for example, high levels of $PM_{2.5}$ in urban areas have been shown to contribute to excess mortality.[3] Given their significance to climate and human health, it is imperative to further investigate the sources and chemical composition of $PM_{2.5}$ in order to adequately develop mitigation strategies, as well as to improve predictive air quality and climate models.

Due to the various sources of $PM_{2.5}$, aerosol composition differs spatially around the United States (US) and globally.[4] Organic matter (OM) can contribute a significant portion of $PM_{2.5}$, and can be derived from both primary and secondary sources. Primary organic aerosols (POA) are directly emitted from both natural and anthropogenic sources. Biogenic POA consists of compounds like pollen and fungal spores,[5] and anthropogenic POA originate from combustion sources. With respect to climate, visibility, and human health, anthropogenic sources are often of the most interest. In urban areas, POA is emitted from combustion of fossil fuel, biomass

burning, and cooking activities. Notably, POA from biomass burning emissions contain some light-absorbing organic species (also known as brown carbon aerosol), contributing to the aerosol direct effect on climate.[6] These anthropogenic activities also release volatile organic compounds (VOCs), which have high vapor pressures and react readily in the atmosphere. Secondary organic aerosols (SOA) are derived from atmospheric oxidation reactions of these VOCs in the presence of oxidants such as hydroxyl radical (OH), nitrate radical ($NO_3$), and ozone ($O_3$).[7] SOA typically contributes much more than POA to $PM_{2.5}$ mass worldwide, with upwards of 90% of the mass of submicron aerosol particles derived from SOA.[8]

Isoprene ($C_5H_8$) is the most abundant nonmethane-VOC in the atmosphere, with emissions of about 600 Tg $yr^{-1}$,[9] and its reaction products have long been of interest to atmospheric scientists. Broadleaf deciduous trees are high emitters of isoprene, and areas that have dense populations of these types of trees can be thought of as hot spots for isoprene and other abundant biogenic volatile organic compounds (BVOCs) such as monoterpenes ($C_{10}H_{16}$) and sesquiterpenes ($C_{15}H_{24}$).[9] Due to high densities of isoprene-emitting trees, the Southeast US and the Amazon rainforest are of particular importance to this research. While both regions are hotspots for isoprene, the industrial development in the Southeast US stands in contrast to the forested landscape of the Amazon. Sulfate, which is derived from fossil fuel burning activities, volcanic eruptions, and sea spray, can have important implications for human health and can be used as a tracer for anthropogenic pollution.[10,11] In the aerosol phase, sulfate is highly reflective, exacerbating the aerosol impacts on climate and visibility.[5,10]

Although atmospheric oxidation of isoprene in urban areas has long been known to contribute to ground-level ozone ($O_3$) production, [12] prior to the early 2000s, isoprene was not thought to yield any SOA that would contribute to $PM_{2.5}$.[13,14] Specifically, chamber experiments

conducted during this time period reacted isoprene with atmospheric oxidants (i.e., OH or $O_3$) that yielded products that were thought to be too volatile to condense onto preexisting aerosols or nucleate into new particles.[13,14] In 2004, new research revealed that atmospheric oxidation of isoprene does in fact yield SOA; however, the mechanism proposed suggested that SOA forms from a series of two cross reactions of isoprene peroxy radicals ($RO_2$) in the gas phase.[15] While this was a monumental breakthrough, researchers involved in this study did not consider the role of acid-catalyzed multiphase (or heterogeneous) chemistry of certain oxidation products from isoprene leading to SOA. This was likely due to lack of knowledge at that time of the complete gas-phase chemistry as a consequence of analytical limitations. However, these authors demonstrated that 2-methyltetrols, which were proposed to be derived from OH-initiated oxidation of isoprene since they had a $C_5$ backbone, had significant mass concentrations in $PM_{2.5}$ collected from the Amazon. Thus, they could serve as important chemical markers for atmospheric isoprene SOA formation. From this initial work, they estimated that up to up to 2 Tg $yr^{-1}$ of isoprene SOA is formed as a result of these 2-methyltetrol products.[15]

Since Claeys et al.[15] re-opened the idea that atmospheric oxidation of isoprene does in fact yield SOA, subsequent chamber studies began investigating the roles of nitrogen oxides ($NO_x$) and sulfur dioxide ($SO_2$) on isoprene SOA formation. Kroll et al. demonstrated that isoprene SOA had higher yields under low-$NO_x$ conditions, likely due to low-volatility organic peroxides condensing onto pre-existing aerosol or nucleating into new particles.[16] The latter was confirmed by chemical characterization studies of Surratt et al.[17-19] Notably, several subsequent chamber studies demonstrated that the presence of $SO_2$, which upon oxidation leads to the formation of acidic sulfate aerosol, enhanced isoprene SOA yields, especially under low-$NO_x$ conditions. Due to the correspondence of high abundances of 2-methyltetrols and $C_5$-alkene

triols measured by gas chromatography/electron ionization mass spectrometry (GC/EI-MS) and organosulfates (OS) measured by liquid chromatography interfaced to electrospray ionization mass spectrometry (LC/ESI-MS) with enhanced SOA growth at higher acidity conditions, it was tentatively proposed that isoprene epoxydiols (IEPOX) may form and then undergo acid-catalyzed multiphase chemistry to yield these SOA constituents.[17] It was later demonstrated by novel online chemical ionization MS (CIMS) techniques that high abundances of IEPOX form in the gas-phase from the OH-initiated oxidation of isoprene under low-$NO_x$ conditions,[20] and in the presence of acidic sulfate aerosol it participates in acid-catalyzed multiphase (reactive uptake) chemistry to yield high abundances of 2-methyltetrols, $C_5$-alkene triols, and OSs.[19,21] Figure 1 summarizes the current gas- and particle-phase reaction mechanisms of IEPOX that are thought to yield most of the isoprene SOA mass in $PM_{2.5}$.[19-23] It is important to note that the original chamber studies (prior to the discovery that atmospheric oxidation of isoprene leads to SOA formation) missed this chemistry because they were conducted under high-$NO_x$ conditions (i.e., high initial levels of NO), low relative humidity (RH) conditions and in the presence of non-acidified ammonium sulfate aerosol particles,[13,14] all of which tends to suppress isoprene SOA formation. Thus, isoprene SOA formation demonstrates the need of laboratory studies to more closely mimic atmospheric conditions of RH, $NO_x$, and aerosol acidity as much as possible.

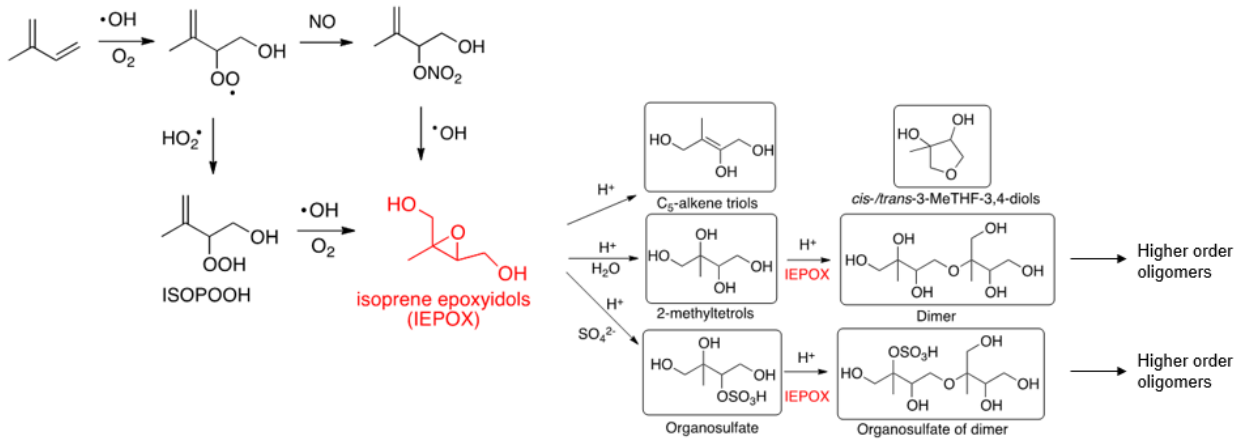


***Figure 1:*** *Low-$NO_x$ isoprene oxidation mechanism that leads to IEPOX that subsequently undergoes acid-catalyzed reactive uptake (multiphase chemistry) with sulfate aerosol.*[19-23] *For simplicity, it should be noted that only one structural isomer is shown for the aerosol-phase reaction products.*

As shown in Figure 1, it was discovered that isoprene hydroxyhydroperoxides (ISOPOOH), which are major gas- phase oxidation products of isoprene, can undergo intermolecular isomerization upon subsequent oxidation with OH radicals to form IEPOX.[20] This is thought to be the main source of atmospheric IEPOX, but it was recently demonstrated that a minor source of IEPOX can come from the intramolecular isomerization of the dihydroxynitrate alkyl radical formed from the OH radical oxidation of isoprene hydroxynitrates formed under higher $NO_x$ conditions.[24] As shown in Figure 2, IEPOX can be present in three isomeric forms: *trans-β*-IEPOX, *cis-β*-IEPOX, and *δ*-IEPOX. *Trans*-β-IEPOX is the most abundant isomer, making up about two thirds of the *β*-IEPOX isomer mass that contributes to 97% of the total IEPOX in the ambient atmosphere, whereas δ-IEPOX accounts for this remaining 3% of the atmospheric pool of IEPOX.[25] *Trans-β*-IEPOX forms a tertiary or secondary carbocation when it undergoes acid-catalyzed ring-opening reactions within wet sulfate aerosol particles.[21] Most prior studies have focused on *β*-IEPOX isomers in terms of their SOA formation potential.[21,22,26]

However, due to the fact that *δ*-IEPOX can produce a primary carbocation once it undergoes acid- catalyzed ring-opening reactions within wet sulfate aerosol, it offers a unique opportunity to examine how epoxide location can affect the multiphase chemistry leading to SOA. Our research group has been able to synthesize *cis*- and *trans-β*-IEPOX isomers as well as *δ*-IEPOX.[21,23]

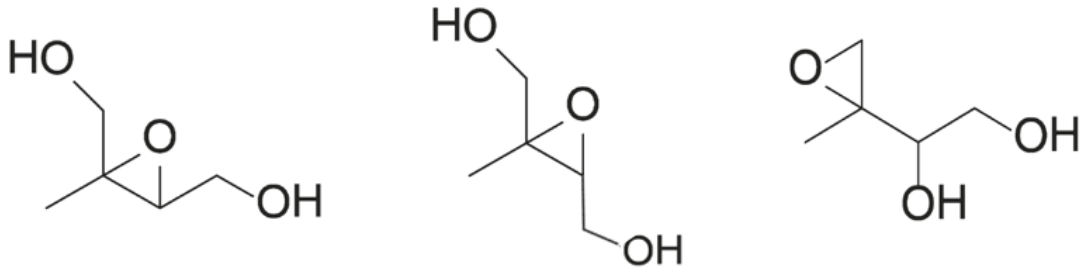


***Figure 2:*** *Isomeric Structures of IEPOX.*

It is believed that the presence of acidic sulfate aerosol from coal combustion enhances the ability of isoprene to make SOA. Therefore, it is important to consider the reaction products of IEPOX with acidic sulfate aerosols. It is expected that the multiphase chemistry of IEPOX on the surface of acidic and wet sulfate aerosol particles will lead to high yields of SOA containing OS, especially under experimental conditions where IEPOX is in excess compared to sulfate aerosol concentrations. This case is especially relevant to the Amazon rainforest, which is a hotspot for isoprene emissions. Lower background levels of sulfate in the Amazon compared to those seen in the Southeast U.S. result in higher IEPOX-to-sulfate (IEPOX:$SO_4^{2-}$) ratios.[27] The IEPOX:$SO_4^{2-}$ ratio is believed to play an important role in the formation of particle-phase OSs and oligomers thereof.[28]

The research presented here is obtained from a series of indoor smog chamber experiments conducted with both *trans*-$\beta$-IEPOX and $\delta$-IEPOX, with special focus on the $\delta$-IEPOX isomer. The primary motivation of these experiments came from field sample data collected during the Southern Oxidant and Aerosol Study (SOAS) in 2013, where it was observed that the organic sulfate measured could only account for roughly half of the total sulfur mass measured on a given day.[29] This prompted questions about the composition of aerosols in the Southeast US, as well as other areas like the Amazon, which are high in isoprene emissions. Recent work that also contributes to this thesis has shown that up to 90% of inorganic sulfur can be converted into organic forms through multiphase chemical reactions of *trans*-$\beta$-IEPOX.[28]

While there have been many studies conducted on IEPOX reactive uptake,[21,22,26,30-34] details of its reactivity and product distribution as a function of sulfate and IEPOX:$SO_4^{2-}$ ratio remains unclear. This research seeks to characterize the aerosol-phase products of IEPOX in the presence of acidified ammonium sulfate aerosol. We expect that the multiphase chemistry of IEPOX on acidic and wet sulfate particles will yield large abundances of OSs, especially at higher IEPOX:$SO_4^{2-}$ ratios. We varied the IEPOX:$SO_4^{2-}$ ratio in a series of chamber experiments, using both isomers of IEPOX. The chamber reactions of *trans*-$\beta$-IEPOX have already been characterized in previous studies published by this group.[21,22,28] The results of $\delta$-IEPOX experiments presented here were collected in tandem with those of the *trans*-$\beta$-IEPOX experiments. By examining these analytical data, the goal of this thesis was to investigate the effect isomeric IEPOX structures and IEPOX:$SO_4^{2-}$ ratio on the sulfur mass balance in $PM_{2.5}$.

# CHAPTER II: EXPERIMENTAL METHODS

## 2.1 Chamber Operation

Varying IEPOX:$SO_4^{2-}$ ratio experiments were conducted at the University of North Carolina at Chapel Hill in an indoor 10-$m^3$ Teflon smog chamber facility under dark and humid (i.e., 50% RH) conditions. A detailed description of this indoor smog chamber facility has been previously described in detail by Lin et al., but is also shown in Figure 3.[21,22] Before the start of each experiment, the chamber was flushed with clean air continuously for at least 24 hours, corresponding to at least 7 chamber volumes. This ensured that preexisting aerosol concentrations and trace gases inside the chamber were below the detection limits of the analytical instrumentation. The night before each scheduled experiment, the chamber was humidified using 2 bubblers operated at 16 L $min^{-1}$. RH and temperature were continuously monitored throughout the experiment using a dew point meter (Omega Engineering Inc.). Chamber aerosol size distributions were measured using a Scanning Electrical Mobility System (SEMS v5.0, Brechtel Manufacturing Inc.) containing a Differential Mobility Analyzer (DMA, BMI) coupled with a mixing condensation particle counter (MCPC Model 1710, BMI). Once the chamber reached a RH of ~ 50%, acidified ammonium sulfate (AAS) seed aerosol was injected into the chamber using a custom atomizer. The AAS seed aerosol was generated by atomizing a solution of 0.06 M $(NH_4)_2SO_4$ and 0.06 M $H_2SO_4$. AAS was injected until the desired aerosol mass concentration was reached (the value of which depended on the targeted IEPOX:$SO_4^{2-}$ ratio for the given experiment).

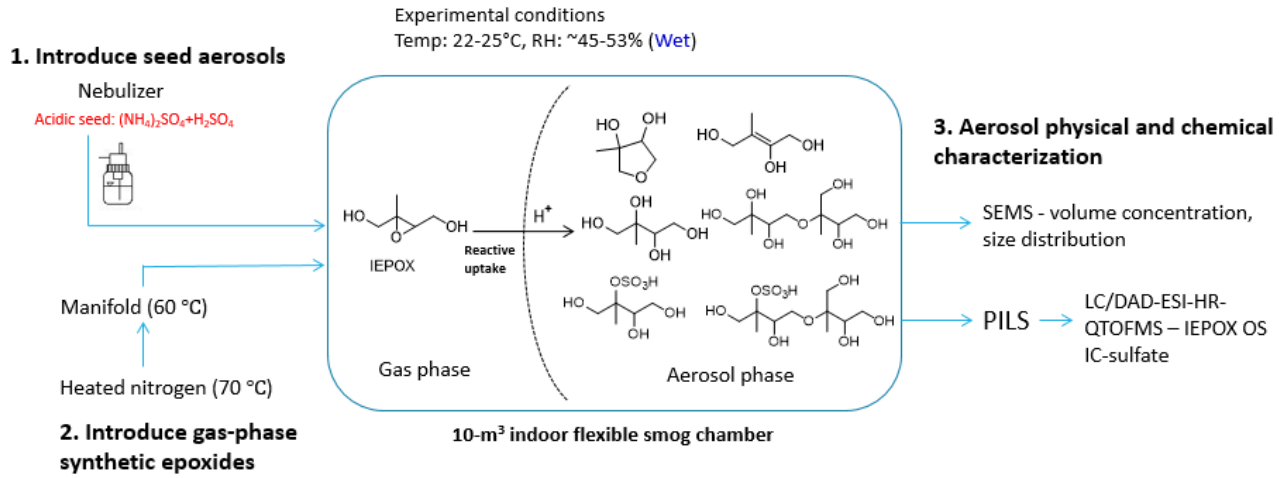


***Figure 3:*** *Experimental setup for generating IEPOX-derived SOA at varying IEPOX:$SO_4^{2-}$ ratios.* *21,22*

Once seed aerosol injection was completed, the chamber was left static for at least 20-30 minutes to ensure uniform mixing of the seed aerosol within the chamber. During this time, a Particle-into-Liquid Sampler (PILS) was connected to the chamber. The PILS sampled chamber air at a flowrate of ~ 12-13 L $min^{-1}$ through a 2.5 μm size cut impactor, upstream of which a carbon strip denuder was located to remove organic vapors (i.e., gas-phase IEPOX). Aerosol particles were allowed to grow by adiabatic mixing of cool sample air flow with steam flow from the PILS condensation chamber (98.5-100 ºC). Once the particles grew to collectible size and were impacted onto a quartz impactor plate, they were transferred by a washflow (0.5-0.55 mL $min^{-1}$) into a debubbler. The resulting sample was deposited into a 2 mL vial held by an autosampler (BMI). Air sampling flowrate and wash flow rate were recorded before and after each experiment. Once air from the chamber had run through the sampling system for a few minutes, 4 PILS samples were collected to capture the background seed aerosol conditions of the chamber. The PILS was paused once these samples were collected.

The δ-IEPOX or *trans*-β-IEPOX was then injected into the chamber for 60 minutes by passing high purity $N_2$ (g) through a glass manifold heated at 75 °C. Depending on the IEPOX:$SO_4^{2-}$ ratio being targeted for a given experiment, the injection manifold contained either 150 or 300 μL of an ethyl acetate solution of authentic δ-IEPOX or *trans*-β-IEPOX. The solution of δ-IEPOX or *trans*-β-IEPOX was synthesized in house according to published procedures.[19,21] The $N_2$ (g) was passed through the manifold at 2 L $min^{-1}$ for 10 minutes, and then at 5 L $min^{-1}$ for the remainder of IEPOX injection. The PILS was restarted at the same time as the $N_2$ (g) flow was initialized. Once this was complete, the manifold was disconnected from the chamber and the reaction occurring inside was allowed to proceed for an additional hour. PILS samples were collected throughout the IEPOX injection and the hour following at 2.5 minute intervals to provide samples at time points throughout the experiment. These PILS samples were stored at 2° C after collection and subsequently analyzed using both ion chromatography (IC) and ultra-performance liquid chromatography interfaced to electrospray ionization high-resolution quadrupole time-of-flight mass spectrometry (UPLC/ESI-HR-QTOF-MS) methods for near real-time quantification of inorganic and organic aerosol constituents. Detailed experimental conditions for the δ-IEPOX experiments are summarized in Table 1 and the *trans*-β-IEPOX experiments are summarized by Riva et al.[28]

***Table 1****: Summary of the δ-IEPOX chamber experiments.*

| Date | IEPOX:$SO_4$ Ratio (dimensionless) | IEPOX injected (ppb) | Seed type[b] | Initial seed volume ($um^3$ $cm^{-3}$) | Maximum aerosol volume after IEPOX injection ($um^3$ $cm^{-3}$) |
|---|---|---|---|---|---|
| **14-Dec 2017** | 3.59 | 266 | AAS | 375.83 | 561.29 |
| **8-Jan 2018** | 3.22 | 296 | AAS | 399.74 | 604.75 |
| **22-Jan 2018** | 28.67 | 454 | AAS | 78.86 | 137.59 |
| **14-Mar 2018** | 42.77 | 524 | AAS | 90.04 | 161.19 |
| **28-Feb 2018** | N/A (wall loss) | N/A[a] | AAS | 400 | 330.51 |
| **26-Mar 2018** | N/A (wall loss) | 300 | N/A[a] | N/A[a] | 0.46 |

[a] N/A indicates that no amount of seed or IEPOX was present in the chamber

[b] AAS is acidified ammonium sulfate seed aerosol

## 2.2 UPLC/ESI-HR-QTOFMS Operating Conditions

Chemical characterization of the PILS samples was performed UPLC/ESI-HR-Q-TOFMS (6520 Series, Agilent) operated in both the negative and positive ion modes. The reverse phase liquid chromatography (RPLC) method utilized in this study was based on the methodology first described by Lin et al.[21,22] PILS samples were immediately analyzed by UPLC/ESI-HR-QTOFMS after the completion of each chamber experiment. PILS samples were analyzed in the positive ion mode the same day of the experiment and in the negative ion mode starting the following day. PILS samples were stored at 2 ºC and dark conditions when not being chemically analyzed. Additional sample preparation was unnecessary before chemical analysis. Prior to UPLC/ESI-HR-QTOFMS analyses, instrument performance was determined by generating calibration curves using authentic standards of 2-methyltetrols and 3-methyletrol sulfates in the positive and negative, respectively, ion modes. In the negative ion mode, five $\mu$L aliquots of the samples and authentic standard mixtures were injected onto the UPLC column

(Waters ACQUITY UPLC HSS T3 column, 2.1 × 100 mm, 1.8 $\mu$m particle size), and eluted at a flow rate of 0.3 mL $min^{-1}$ with a mobile phase mixture of methanol containing 0.1% acetic acid (w/w) (LC-MS CHROMASOLV-grade, Sigma- Aldrich) and water containing 0.1% acetic acid (w/w) (LC-MS CHROMASOLV-grade, Sigma-Aldrich). In the positive ion mode, the mobile phase mixture consisted of methanol containing 0.1% formic acid (w/w) (LC/MS CHROMASOLC-grade, Sigma-Aldrich) and water containing 0.1% formic acid (w/w) (LC/MS CHROMASOLV-grade, Sigma-Aldrich).

**2.3 IC Operating Conditions**

After the completion of each chamber experiment and UPLC/ESI-HR-QTOFMS analysis, selected PILS samples were analyzed using IC (ICS 3000, Thermo Fisher). Compounds were quantified using standards prepared in-house (and a 7-point calibration curve generated in the range of 1-200 μmol $L^{-1}$). A 25 μL aliquot of each sample and authentic standard mixture were analyzed by IC, using an IonPac AS11-HC guard column (2×50 mm, Thermo Scientific) and anion-exchange column (2×250 mm, Thermo Scientific). Samples were analyzed at a flow rate of 0.4 ml $min^{-1}$.[35] A potassium hydroxide (KOH) gradient elution scheme was utilized is described as follows. The temperature of the conductivity detector (Dionex) that interfaced to the IC was set at 30 °C. The 35-min KOH gradient elution scheme utilized for all experiments is as follows: 1.00 mM KOH increased to 30.00 mM KOH during the first 25 min, ramped up to 84.00 mM KOH at 30 min and held until 30.1 min, and decreased back to 1.00 mM over the next 4.9 minutes (total time 35 min).

Once IC analyses were completed, a PILS dilution factor was calculated based on the data (further explanation of data analysis can be found in Appendix II). In an ideal experiment, the concentration of lithium bromide (LiBr) in the PILS samples should be identical to that of the

wash flow within the PILS. However, due to the addition of water from condensation to the sample aliquots, it is necessary to calculate the factor by which samples were diluted within the PILS. This factor differs on a sample-by-sample basis, and can be calculated using the following formula[28]:

$$dilution\ factor = \frac{[Br^-]_{wash\ flow}}{[Br^-]_i}$$

Where "i" denotes the bromide ($Br^-$) concentration measured in each sample by IC analysis and "wash" denotes the $Br^-$ concentration measured in the wash flow.[28] Sample concentrations were corrected by multiplying the measured concentration by the corresponding dilution factor.

## CHAPTER III: RESULTS AND DISCUSSION

The main research question this thesis sought to answer was whether or not *trans-β*-IEPOX consumes more inorganic sulfate aerosol than *δ*-IEPOX. If this was the case, we also wanted to know why this effect was seen in our series of chamber studies, and whether the possible lower yield of SOA from *δ*-IEPOX was tied to a lower conversion of inorganic sulfate to OS. Inorganic sulfate is a large component of $PM_{2.5}$,[9] so varying concentrations of this could have important ramifications for SOA formation from acid-catalyzed multiphase chemistry of IEPOX. A summary of the concentrations of the species of interest as well as the overall SOA mass produced and percentage (%) of inorganic sulfate consumed for each experiment is presented in Table 2. All concentrations presented in Table 2 and subsequent figures have been corrected for wall loss. The plots presented in this section portraying the *δ*-IEPOX chamber experiments (Table 2) are from 12/14/17 (IEPOX:$SO_4^{2-}$ ratio of ~ 3.6) and 1/22/18 (IEPOX:$SO_4^{2-}$ ratio of ~ 28.7), and those from the *trans-β*-IEPOX chamber experiments are from 12/4/17 (IEPOX:$SO_4^{2-}$ ratios of ~ 1.6) and 11/8/17 (IEPOX:$SO_4^{2-}$ ratio of ~ 13.6). Plots from the additional experiments conducted on 1/8/18 (IEPOX:$SO_4^{2-}$ ratio of ~ 3.2 and 3/14/18 (IEPOX:$SO_4^{2-}$ ratio of ~ 42.8) are presented in Appendix I.

***Table 2:*** *Experimental Summary of SOA Mass Produced, Sulfate Consumed and Organosulfate Products Formed from the Acid-Driven Reactive Uptake of δ-IEPOX onto Acidic Sulfate Aerosol.*

| **Date of Expt. (IEPOX:$SO_4^{2-}$ ratio)** | **SOA Mass Concentration Produced[a] (μg $m^{-3}$)** | **IEPOX-OS Monomer[b] (μg$SO_4^{2-}$ $m^{-3}$)** | **IEPOX-OS Dimer[b] (μg$SO_4^{2-}$ $m^3$)** | **IEPOX-OS Trimer[b] (μg$SO_4^{2-}$ $m^{-3}$)** | **% of Inorganic $SO_4^{2-}$ Converted to OS[c]** |
|---|---|---|---|---|---|
| **12/14/17 (3.6)** | 330.22 | 26.37 | 0.90 | 0.074 | 26.8% (95.10 μg $m^{-3}$) |
| **1/8/18 (3.2)** | 394.06 | 33.33 | 1.53 | 0.23 | 28.6% 119.23 μg $m^{-3}$) |
| **1/22/18 (28.7)** | 114.11 | 60.73 | 2.12 | 0.32 | 53.9% (38.1 μg $m^{-3}$) |
| **3/14/18 (42.8)** | 124.95 | 40.39 | 1.43 | 0.17 | 59.7% (27.5 μg $m^{-3}$) |

[a] The total SOA mass concentration includes the SOA volume growth (maximum-starting value) and the sulfate mass consumed, which is multiplied by the density of isoprene SOA

[b] These concentrations represent the maximum concentration of the compound in the chamber over the course of the experiment.

[c] Calculated from sulfate consumption measured by PILS-IC over the first hour of IEPOX injection.

As evident in Table 2 above, there was a larger % of inorganic sulfate consumption seen in the high ratio case compared to that of the low ratio. The amount of sulfate converted into OS in the low ratio experiments was far less than in the high ratio ones, with at most 28.6% conversion, compared to a maximum of 59.7% conversion in the high ratio case. This trend holds for experiments conducted with *trans-β*-IEPOX as well, with 33.3% of inorganic sulfate converted to OS in the low ratio case, and 87.4% conversion of inorganic sulfate in the high ratio case. Interestingly, the conversion of inorganic sulfate to OS is always higher when *trans-β*-

IEPOX is present in the chamber, regardless of the ratio. The trend of lower sulfate consumption in the low ratio case compared to the high ratio case holds in situations where *trans-β*-IEPOX is present as well.

### 3.1 Low Ratio Experiments: Simulated Southeast US Conditions

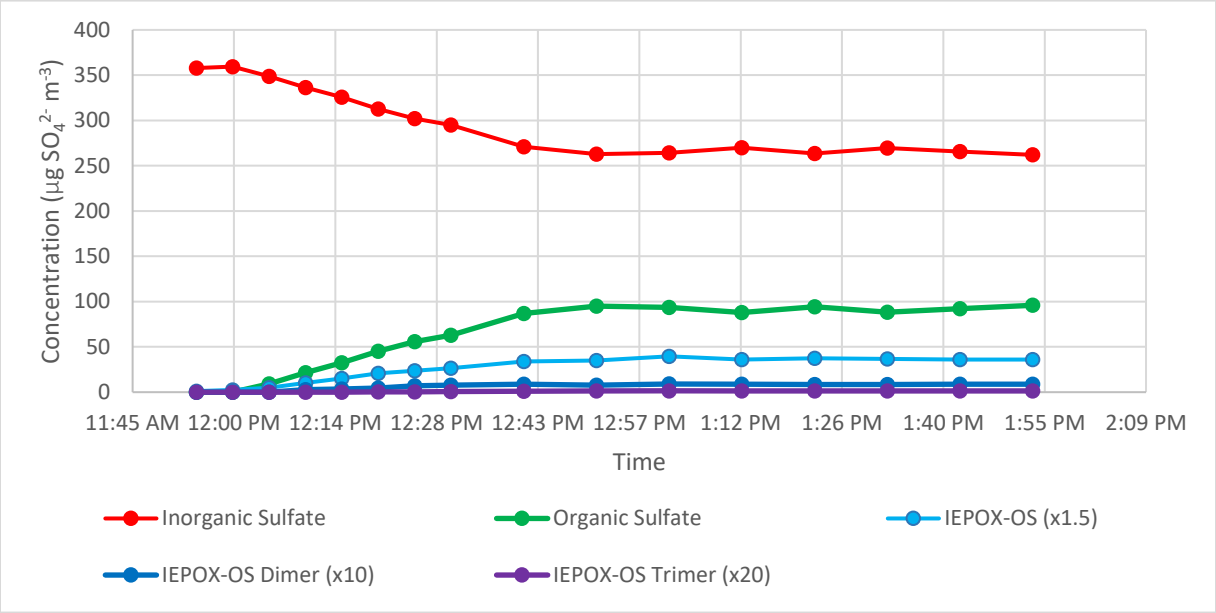


***Figure 4:*** *Simulated Southeast US conditions with δ-IEPOX yielding SOA. (12/14/17, IEPOX:$SO_4^{2-}$ ratio ~3.6)*

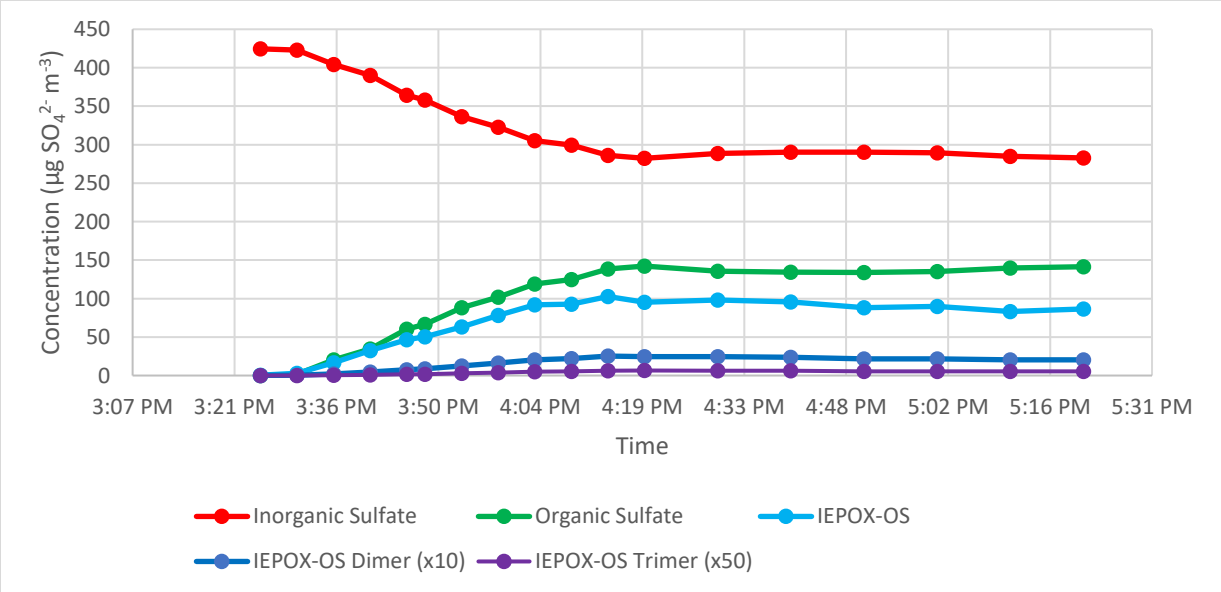


***Figure 5****: Simulated Southeast US conditions with* trans-β*-IEPOX yielding SOA. (12/4/17, IEPOX:$SO_4^{2-}$ ratio ~1.6)*

As shown in Figures 4 and 5, once *δ*-IEPOX and *trans-β*-IEPOX, respectively, were injected into the smog chamber (at 11:54 am local time for Figure 4, and 3:25 pm local time for Figure 5), conversion (or consumption) of inorganic sulfate to OS can be observed using these low IEPOX:$SO_4^{2-}$ratios. Over the course of the first hour of each experiment, during which IEPOX was injected into the chamber, the IEPOX-OS monomer grew relatively fast, followed by the IEPOX-OS dimer and trimer; these particle-phase reaction products measured by the PILS-UPLC/ESI-HR-QTOFMS method clearly indicated that the rapid decrease of inorganic sulfate ($SO_4^{2-}$) measured by the PILS-IC method yields organic forms. However, the growth of OS compounds occurs at a quicker rate in experiments that used *trans-β*-IEPOX (Figure 5) compared to those that used *δ*-IEPOX (Figure 4). The rate of OS growth, which was 128.82 μg total OS $m^{-3}$ $hr^{-1}$ with *trans-β* IEPOX and 32.57 μg total OS $m^{-3}$ $hr^{-1}$ with δ-IEPOX, was calculated using the following formula:

$$Growth\ rate\ of\ OS\ [\mu g\ m^{-3} hr^{-1}] = \frac{[monomer]_{max} + [dimer]_{max} + [trimer]_{max}}{t_{max} - t_0}$$

Where $t_{max}$ denotes the time at which the OS species were at their maximum concentration and $t_0$ denotes the time at which IEPOX was introduced in the chamber. Values of OS growth rates are denoted in Table 3.

***Table 3:*** *Growth rate of organosulfate species in low ratio experiments.*

| Date | Ratio | Growth Rate of OS (μg OS $m^{-3}$ $hr^{-1}$) |
|---|---|---|
| **12/14/17 (δ-IEPOX)** | 3.57 | 32.57 |
| **1/8/18 (δ-IEPOX)** | 3.22 | 29.06 |
| **12/4/17 (*trans-β* IEPOX)** | 1.56 | 128.82 |

At low IEPOX:$SO_4^{2-}$ ratios, the % of sulfate converted into OS is also slightly higher in the *trans-β*-IEPOX experiment (33.3% on average) than the *δ*-IEPOX experiment (27.7% on average), indicating the importance of the location of the epoxide moiety within the isoprene backbone. Based on the isomeric structural differences and the carbocations they form under acid-catalyzed ring-opening reactions, there could be higher order oligomers or other unknown compounds forming rapidly once the monomer has formed, thereby keeping the overall IEPOX-OS monomer concentrations lower during the *δ*-IEPOX experiments than in cases when *trans-β*-IEPOX was present in the chamber.

Based on the comparison between low IEPOX:$SO_4^{2-}$ ratio experiments conducted with *δ*- and *trans-β*-IEPOX, a clear distinction between mass closure emerges. At the conclusion of the low IEPOX:$SO_4^{2-}$ ratio experiment with *trans-β*-IEPOX, 33.3% of inorganic sulfate had been consumed, compared to an average of 27.7% in the case where *δ*-IEPOX was used. In all cases, the inorganic sulfate consumption stabilized after the first hour, resulting in the final inorganic sulfate consumption, presented in Table 2. It is interesting to note that the growth of OS plateaus after this first hour, as does the decay of inorganic sulfate. Based on Riva et al.[28], it has been hypothesized that the aerosol morphology changes from a homogenous particle to a phase separated one. This would result in the aqueous inorganic sulfate to be sequestered in the core of the particle, where it is inaccessible to further conversion to OS by IEPOX due to the viscous SOA shell of the particle that formed during the 1$^{st}$ hour. This SOA shell is thought to become highly viscous, which prevents IEPOX from partitioning and reacting with the sulfate core.[28] Microscopy images were provided by Dr. Andrew Ault's research group at the University of Michigan (which are located in Appendix I) that indicate this trend appears to hold for δ-IEPOX as well. This would explain why the decay of inorganic sulfate gradually ceases over the course

of low ratio experiments. Another possibility is that particle acidity could be changing throughout the experiment, although this may not be the biggest factor at play here. More discussion of this possibility will occur in the next section concerning the high ratio experiments.

As mentioned above, the carbocation structure in the *trans-β*-IEPOX case (either a secondary or tertiary carbocation) provides a more stable intermediate than the primary carbocation formed from acid-catalyzed ring-opening of *δ*-IEPOX. It is possible that our LC/ESI-HR-QTOFMS method is unable to detect certain organic sulfate forms, such as diaklylsulfates. This could account for the remaining OS mass that cannot be explained by the IEPOX-OS monomer and oligomers.

### 3.2 High Ratio Experiments: Simulated Amazonian Conditions

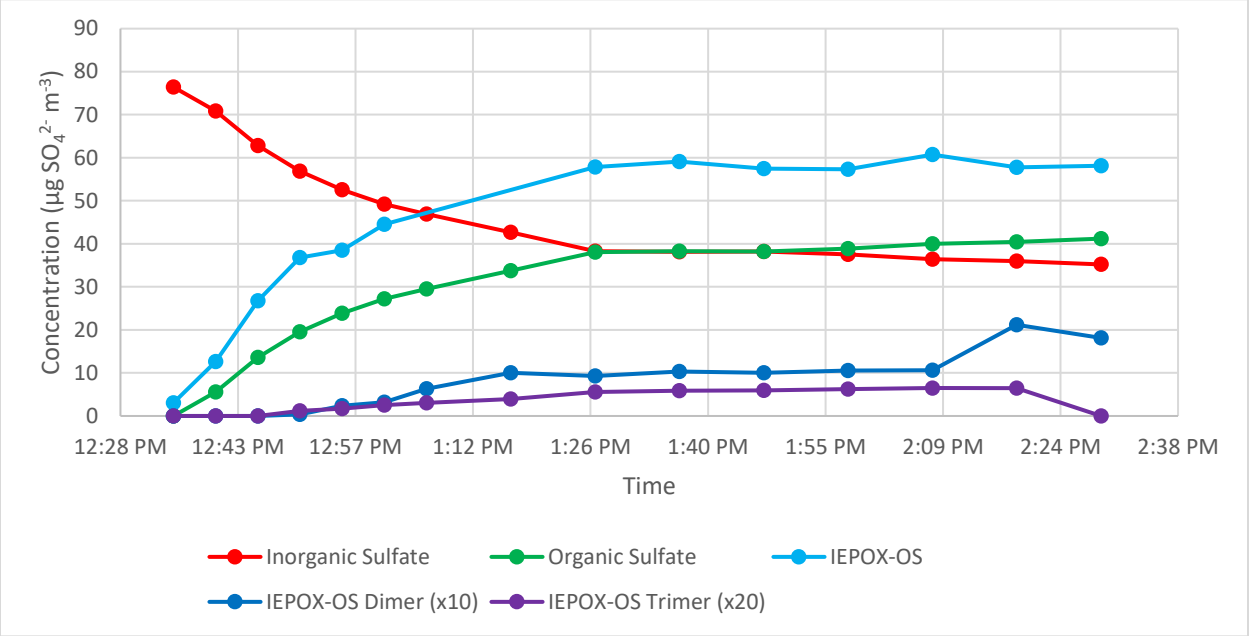


***Figure 6:*** *Simulated Amazonian conditions with δ-IEPOX yielding SOA on 1/22/18 (IEPOX:$SO_4^{2-}$ ~28.7)*

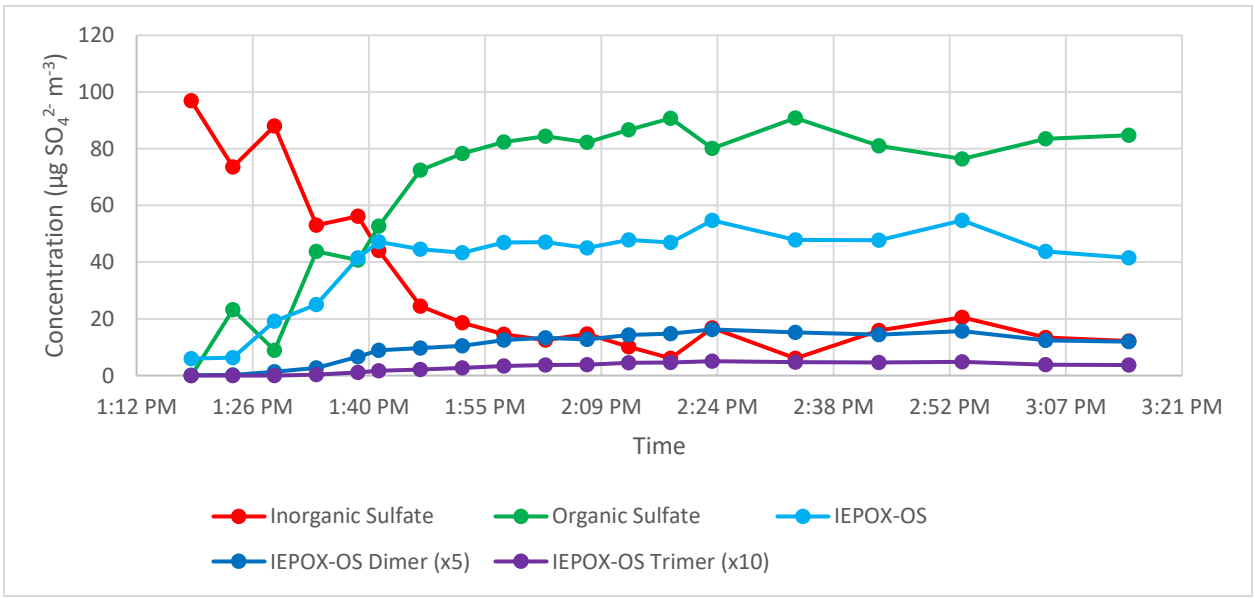


***Figure 7:*** *Simulated Amazonian conditions with* trans-β-*IEPOX yielding SOA on 11/8/17 (IEPOX:$SO_4^{2-}$ ~13.6)*

As with the low ratio experiments, rapid conversion of inorganic $SO_4^{2-}$ into organic forms occurs in the high ratio chamber experiments (Figures 6 and 7). In the case where *trans-β-*IEPOX (IEPOX:$SO_4^{2-}$ ratio of ~ 28.7) is present in the chamber (Figure 7), the amount of

inorganic sulfate consumed over the course of the experiment is 87.44%. Conversely, the inorganic sulfate consumption with $\delta$-IEPOX at a high IEPOX:$SO_4^{2-}$ ratio (~ 28.7) is only 53.92%. This lower conversion of inorganic sulfate into OS is much more pronounced than in the low ratio cases, but the % of sulfate consumed during the high ratio $\delta$-IEPOX experiment shown in Figure 5 is larger than the corresponding low ratio $\delta$-IEPOX experiment shown in Figure 4. Growth rates of OS species during high ratio experiments are summarized in Table 4.

***Table 4:*** *Growth rate of organosulfate species in high ratio experiments.*

| Date | Ratio | Growth Rate of OS (μg OS $m^{-3}$ $hr^{-1}$) |
|---|---|---|
| **1/22/18 (δ-IEPOX)** | 28.68 | 40.08 |
| **3/14/18 (δ-IEPOX)** | 42.77 | 22.08 |
| **11/8/17 (*trans*-β IEPOX)** | 13.61 | 70.66 |

However, as shown in Figure 6, the concentration of the IEPOX-OS monomer exceeds that of the total organic sulfate determined from the IC measurement of sulfate decay, meaning the mass closure would be greater than 100%. We hypothesize that in this experiment that OS products that form are more prone to hydrolysis during the time it takes to analyze them by IC. Typically, these samples were analyzed by IC 2 days after each of these experiments were completed; however, the UPLC/ESI-HR-QTOFMS analyses were conducted immediately after the experiment and within 24 hours of completion of the experiment. It is possible that certain isomers of IEPOX-OS monomers and corresponding OS oligomers from $\delta$-IEPOX in this high IEPOX:$SO_4^{2-}$ ratio experiment are prone to hydrolysis during sample storage. Past studies by Elrod and colleagues have shown that tertiary OSs are more prone to hydrolysis than primary OSs.[36] Our study results suggest a need to store 2-methyltetrol sulfates and 3-methyltetrol sulfates in PILS-like vial conditions collected from typical experiments and to analyze them

immediately after collection as well as over time to examine if they decay back into inorganic sulfate when stored. Furthermore, it may even be necessary to develop isomer-specific standards for comparison, as this effect is not seen in chamber experiments run with *trans-β*-IEPOX. If this effect is indeed the reason for this overestimation of IEPOX-OS in the high ratio case, we may be overestimating concentrations of IEPOX-OS from *δ*-IEPOX in the low ratio case as well. This would mean the observed low ratio mass closure may in fact be even less than estimated in this thesis. Lastly, future experiments should run IC analysis first (immediately after the experiment) followed by UPLC/ESI-HR-QTOFMS (rather that the reverse); these same PILS vials should be reanalyzed using both analytical techniques 2-3 days later by these same techniques to see how they might degrade during storage. If we are able to understand how samples degrade over time, then past data could be possibly corrected for this effect.

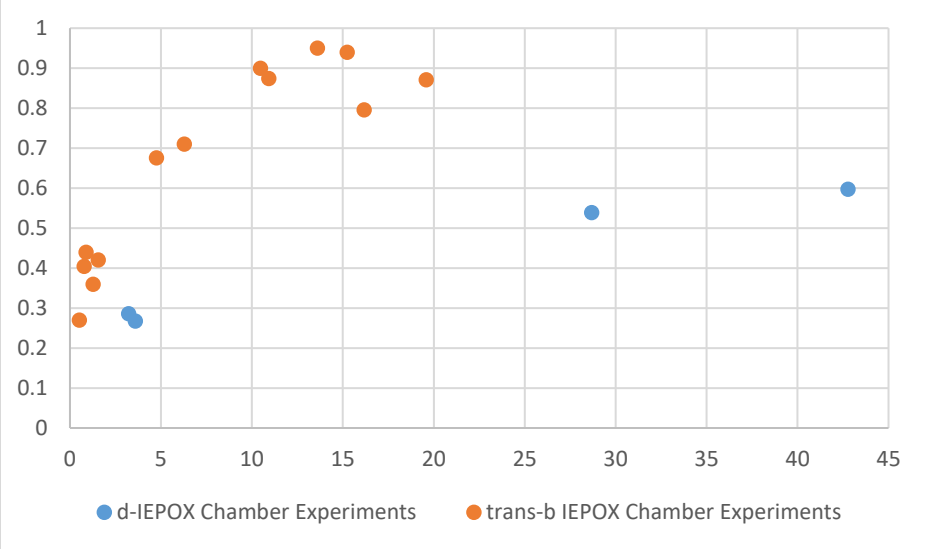


***Figure 8:*** *Sulfate consumed versus IEPOX:$SO_4^{2-}$ ratio.*

Based on the IEPOX:$SO_4^{2-}$ ratio in the *trans-β*-IEPOX experiments, the sulfate reacted at a given ratio increased with an increase in the ratio. In the series of experiments conducted with *δ*-IEPOX, this effect seems to be much less pronounced, with less sulfate consumption at higher

ratios compared to the *trans-β*-IEPOX experiments (see Figure 8). This effect is likely due to the hydrolysis of certain OS products formed under this particular experiment with *δ*-IEPOX during sample storage before IC analyses. These experiments will need to be re-examined in the future where IC and UPLC/ESI-HR-QTOFMS are run immediately after the completion of the experiment and then a few days later, as mentioned previously. This effect should be investigated in a similar fashion to the *trans-β*-IEPOX experiments in the future, where a wider range and number of IEPOX:$SO_4^{2-}$ ratios have been more thoroughly investigated, to better understand and characterize this effect. Based on measurements conducted in the *trans-β*-IEPOX experiments, which are presented in Riva et al. (2019, submitted for publication), the case of a high IEPOX:$SO_4^{2-}$ ratio is the direction in which the Southeast US is heading.[28] While a high IEPOX:$SO_4^{2-}$ ratio in this study is used to represent the simulated Amazonian conditions, it is worth investigating a wider range of IEPOX:$SO_4^{2-}$ ratios in order to better understand the differences in sulfate consumption.

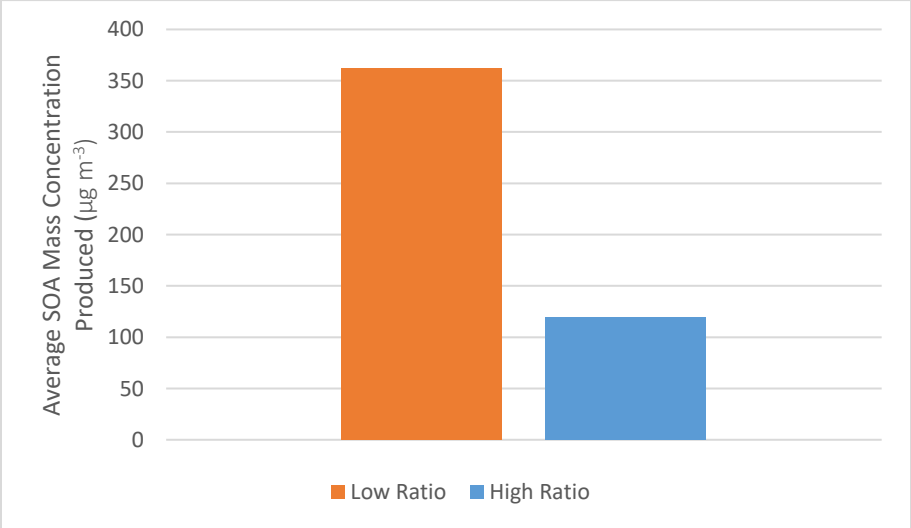


***Figure 9:*** *Average SOA mass concentrations produced with δ-IEPOX.*

As shown in Figure 9, the average SOA mass concentration produced for low ratio experiments was roughly 3 times larger than that of the high ratio experiments. In order to calculate SOA mass concentration, a density of 1.25 g $cm^{-3}$ was assumed to convert volume concentrations measured by the SEMS-CPC into mass concentrations. This density is based on prior data published by Kroll *et al.*[16] This resulted in SOA mass concentrations that were much larger in the case of a low IEPOX:$SO_4^{2-}$ ratio. In the future, the density of *δ*-IEPOX-derived SOA particles should be investigated further. It could be that the density assumed by many atmospheric scientists when conducting experiments with IEPOX isomers could in fact be an underestimate. A more robust estimate for *δ*-IEPOX-derived SOA density could improve measurements of δ-IEPOX SOA mass concentrations.

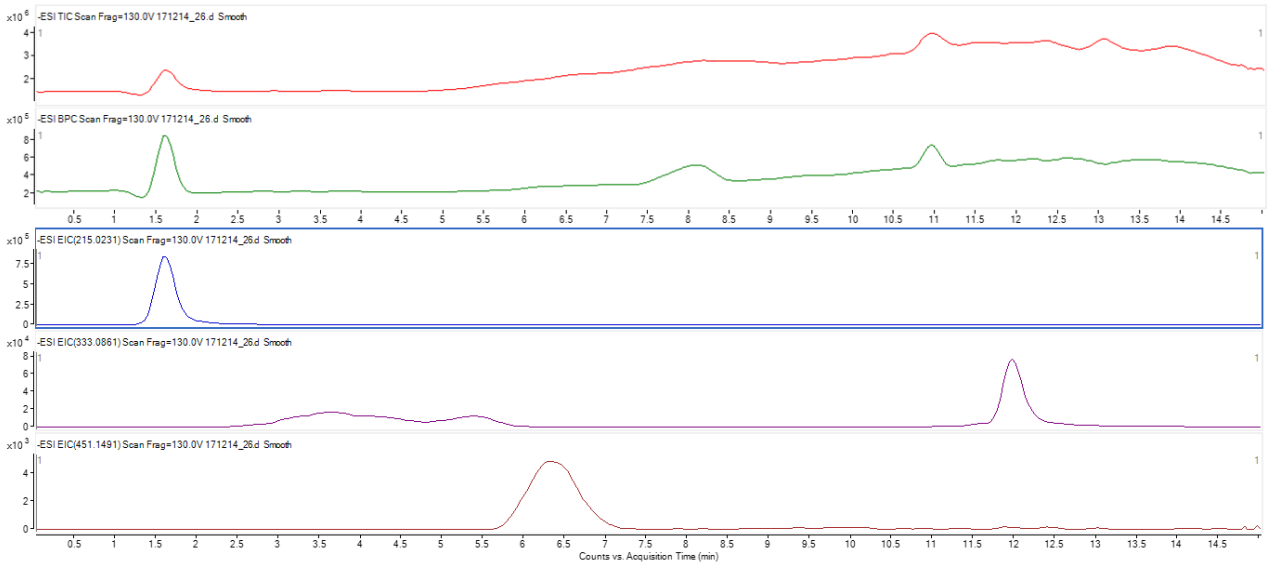


***Figure 10:*** *Negative Ion Mode Chromatograms for δ-IEPOX Low Ratio Case (12/14/17) – from top: TIC, BPC, EIC (m/z = 215.0231), EIC (m/z = 333.0821), EIC (m/z = 451.1491)*

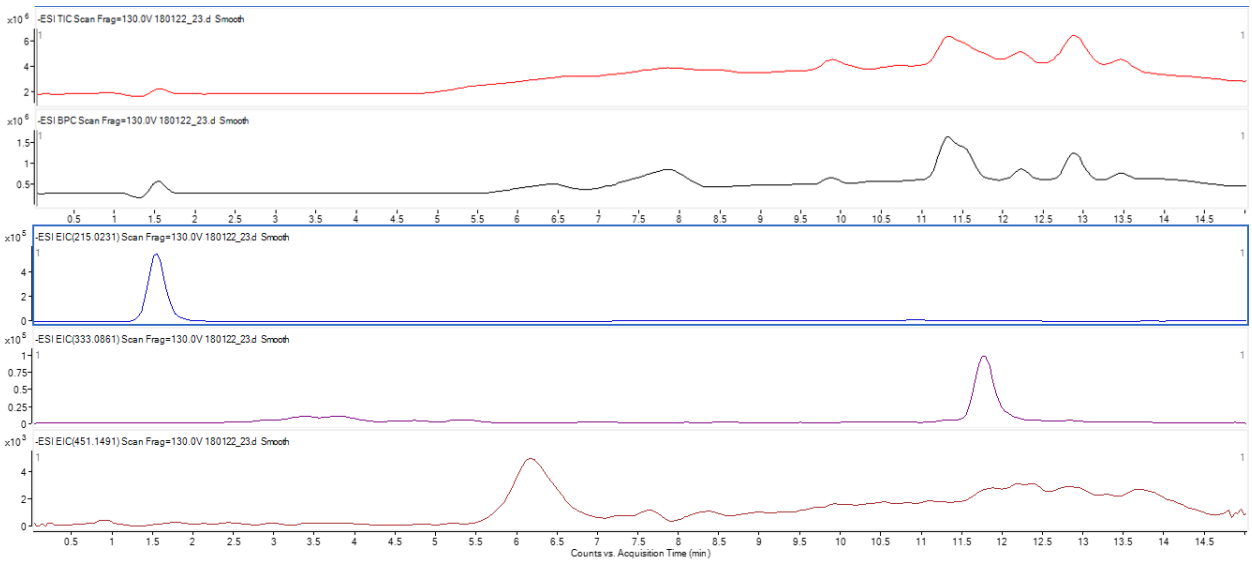


***Figure 11****: Negative Ion Mode Chromatograms for δ-IEPOX High Ratio Case (1/22/18) – from top: TIC, BPC, EIC (m/z = 215.0231), EIC (m/z = 333.0821), EIC (m/z = 451.1491)*

Based on the research presented here, *trans-β*-IEPOX consumes more inorganic sulfate than *δ*-IEPOX, resulting in higher sulfate mass closure in the low ratio case. This lower conversion with *δ*-IEPOX was likely the result of lower conversion of inorganic $SO_4^{2-}$ to OS, as well as the formation of more unknown products and higher order oligomers (presumably non-S containing products) during the chamber studies. Based on chromatographic data (Figures 10 and 11), these larger products can be detected using the analytical techniques used herein. However, as mentioned previously, it may be necessary for isomer-specific standards to be tested as well to corroborate this finding. Future iterations of this work could include hydrophilic interaction liquid chromatography HILIC analysis, which is discussed in the next chapter, especially since it was recently demonstrated to resolve several more IEPOX-OS isomers compared to the RPLC column utilized in the present work.[37]

## CHAPTER IV: CONCLUSIONS AND LIMITATIONS

The importance of isomeric structures of IEPOX can now be seen as a significant driver in determining SOA product distribution, SOA mass produced, and % of inorganic sulfate consumed during the simulated chamber environments. Although *δ*-IEPOX only makes up about 3% of IEPOX found in the ambient atmosphere,[20] the observed differences in product distribution are significant enough to warrant further investigations, especially since it could be hypothesized that other VOCs that are oxidized in the atmosphere could produce terminal epoxide structures like *δ*-IEPOX. These results could serve as a model for understanding the multiphase chemistry of epoxides produced from the atmospheric oxidation of other VOCs. Based on these experiments it is evident that *δ*-IEPOX consumes less inorganic sulfate than *trans-β*-IEPOX. This is possibly due to higher order oligomers and unknown products forming (including non-OS products) in the chamber faster than the IEPOX-OS monomer forms after introduction of *δ*-IEPOX into the system. This could help explain the slower growth of the monomer in *δ*-IEPOX experiments compared to the *trans*-β-IEPOX experiments, as well as the lower sulfate mass closure in the *δ*-IEPOX experiments. If other compounds that we cannot reliably measure (whether due to the lack of authentic standards, analytical limitations, or both) are forming in the chamber along with the IEPOX-OS monomer, the sulfate mass closure estimate presented in this thesis may not be accurate for δ-IEPOX. However, it has also been demonstrated the hydrolysis of OS may occur during sample storage, which needs to be more

systematically examined in the future in order to determine if this effect explains the > 100 % sulfate mass closure observed in the high $\delta$-IEPOX:$SO_4^{2-}$ ratio experiments.

A particularly interesting finding lies in the data generated in the high ratio experiments using $\delta$-IEPOX. The concentration of the IEPOX-OS monomer overtakes that of the estimated OS budget, based on IC data. While this was initially thought to be due to differing response factors between 2- and 3-methyltetrol OS standards (the latter of which was used for analysis in this research), the standards' response factors only differ by a factor of ~ 1.07. A more likely reason for this observed anomaly could be due to hydrolysis of OSs back into inorganic sulfate during sample storage. Samples were analyzed by IC ~ 2 days after collection, and following UPLC/ESI-HR-QTOFMS analysis, in which time hydrolysis reactions of OS could have occurred. In future research with $\delta$-IEPOX (and likely with $\beta$-IEPOX isomers), IC analyses should be conducted the same day of the chamber experiment as well as after UPLC/ESI-HR-QTOFMS analyses in order to examine the potential degradation and hydrolysis of the SOA products over time. Additionally, authentic standards should be stored in aqueous solution and measured for hydrolysis rates to determine whether the abundant IEPOX-OS monomers measured in this work are causing this effect, or if it is the result of the hydrolysis of other as yet unknown products or oligomeric OSs.

In all cases described herein, it is worth noting that not all of the inorganic sulfate was consumed over the course of the experiment (although the high ratio case consumed more inorganic sulfate than the low ratio case). Based on microscopy images that are included in Appendix I, it is apparent that the particles forming throughout $\delta$-IEPOX experiments develop a core-shell morphology, resulting in an aqueous sulfate core and an SOA shell. These images suggest that the IEPOX SOA shell becomes very viscous as the reaction proceeds, which

prevents additional gas-phase IEPOX from partitioning into the aqueous sulfate core. In this phase-limited state, the viscous SOA shell shuts down the further uptake of IEPOX onto the particle, and dramatically slows the conversion of inorganic sulfate to organic forms. Future iterations of this research should look at aerosol acidity in addition to the IEPOX:$SO_4^{2-}$ ratio as a variable. As aerosol acidity is heavily impacted by inorganic sulfate concentrations, there is likely a difference in SOA acidity between the Southeast US and the Amazon. Based on current atmospheric models, only $SO_4^{2-}$ is treated as an important factor in estimating aerosol pH.[38] However, we have demonstrated here that there is noteworthy conversion of inorganic sulfate to OS (or organic sulfur) forms, which may significantly impact estimates of aerosol pH in isoprene-dominated regions (i.e. the Amazon). If the OSs formed from the acid-driven multiphase chemistry of IEPOX are as acidic as bisulfate, then it is likely important to consider the pKas of these compounds in atmospheric chemistry models to more accurately estimate aerosol pH. Currently, pKas of these IEPOX-derived OSs are unknown.

Additionally, there are limitations with the UPLC method used for quantifying the IEPOX-derived OS oligomers. While the methods used for this research are sufficient to look at both IEPOX-OS and 2-methyltetrols, this requires running the MS instrument in both the positive ion (to identify 2-methyltetrols) and negative ion (to identify IEPOX-OS monomers and oligomers thereof) modes. With many PILS samples collected during each chamber experiment, the RPLC method used in the present study can become quite time- and resource-intensive. In tandem with this research, other members of our lab developed a HILIC method for analyzing samples containing highly polar and water-soluble compounds.[37] By using this newly developed HILIC method, future researchers will only have to analyze their samples in the negative ion mode, rather than using both ion modes. Additionally, although it is possible to see the

compounds of interest using the RPLC column, the HILIC method allows users to resolve more chromatographic peaks of the OSs and their associated isomers, which likely increases accuracy in quantification. The advantages of the HILIC method would be well suited for investigating further questions related to isoprene-derived SOA formation, especially in terms of the effect reported here.

Several unexplored questions remain after this research was concluded and should be addressed in future studies about IEPOX isomers. The first of these is the effect of aerosol pH, which was not able to be fully investigated here. In future iterations of work with $\delta$-IEPOX, researchers should investigate how the pH of products formed changes over time, which could help explain why the decay of inorganic sulfate flattens out well before the end of an experiment. Additionally, there needs to be a more in-depth look at phase morphology in future work with $\delta$-IEPOX.

A larger-scale implication of the results of this thesis has to do with air quality policy. When looking solely at $SO_4^{2-}$ conversion in the $\delta$-IEPOX experiments, the high ratio conditions indicate a higher conversion of $SO_4^{2-}$ into OS compounds. However, it is important to also look at mass concentration produced and not just % conversion. Without knowledge of the actual SOA mass produced, it may appear that areas with lower $SO_4^{2-}$ concentrations end up producing more OS. In fact, although the conversion rate is higher in the high ratio case, the actual SOA mass produced is much less, meaning that areas with lower $SO_4^{2-}$ concentrations (i.e. one where IEPOX is present in excess of $SO_4^{2-}$) also have lower production of SOA. This is supported by ambient measurements (SOAS) and chamber measurements quantified here. Standards for criteria pollutants, including $SO_2$, should continue to be monitored and enforced at or below current levels to ensure the health and safety of populations in areas with higher levels of

anthropogenic emissions. In cleaner environments with less anthropogenic pollution, there would be less total SOA production, protecting populations from exposure to PM and other potentially harmful aerosol products.

## APPENDIX I: ADDITIONAL PLOTS

***Table 5:*** *Estimated SOA Yields from Acid-Catalyzed Reactive Uptake of δ-IEPOX.*

| Experimental Date | IEPOX:$SO_4^{2-}$ Ratio | Injection Efficiency (%) | Estimated SOA Yield (%) |
|---|---|---|---|
| **12/14/17** | 3.59 | 88.67 | 25.72 |
| **1/8/18** | 3.22 | 98.67 | 27.58 |
| **1/22/18** | 28.68 | 75.67 | 5.21 |
| **3/14/18** | 42.77 | 87.33 | 4.94 |

Note that SOA yield was calculated using the amount of IEPOX injected into the chamber as the amount of VOC reacted, as we could not accurately estimate its reactive loss during the chamber experiments. The volume of IEPOX injected was based on the weight difference in the manifold before and after injection. This likely means that the yields presented above are underestimates compared to the actual yields, since injection efficiency is not 100%.

***Table 6:*** *Experimental Summary of SOA Mass Produced, Sulfate Consumed and Organosulfate Products Formed from the Acid-Driven Reactive Uptake of trans-β-IEPOX onto Acidic Sulfate Aerosol.*

| Date of Expt. (IEPOX:$SO_4^{2-}$ ratio) | IEPOX-OS Monomer ($\mu g SO_4^{2-}\ m^{-3}$) | IEPOX-OS Dimer ($\mu g SO_4^{2-}\ m^{3}$) | IEPOX-OS Trimer ($\mu g SO_4^{2-}\ m^{-3}$) | % of Inorganic $SO_4^{2-}$ Converted to OS |
|---|---|---|---|---|
| **12/4/17 (3.6)** | 102.72 | 2.53 | 0.13 | 33.3% |
| **11/8/17 (13.6)** | 54.73 | 2.96 | 0.46 | 87.4% |

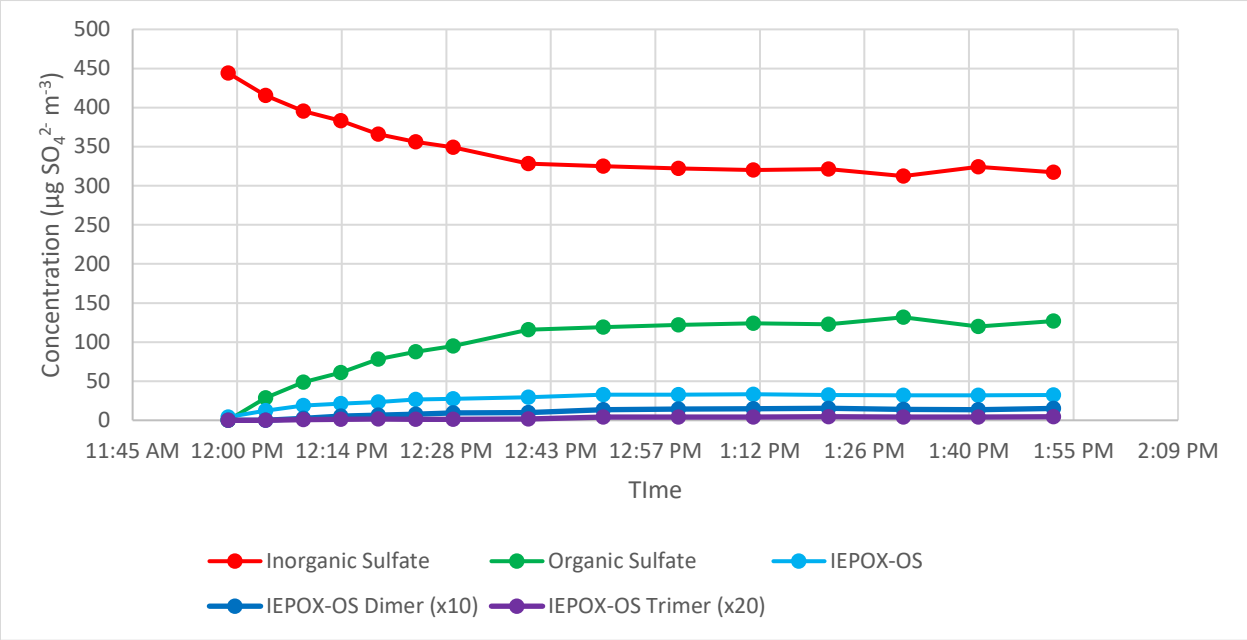


***Figure 12:*** *Simulated Southeast US Conditions with δ-IEPOX on 1/8/18 (IEPOX:$SO_4^{2-}$ ~3.2)*

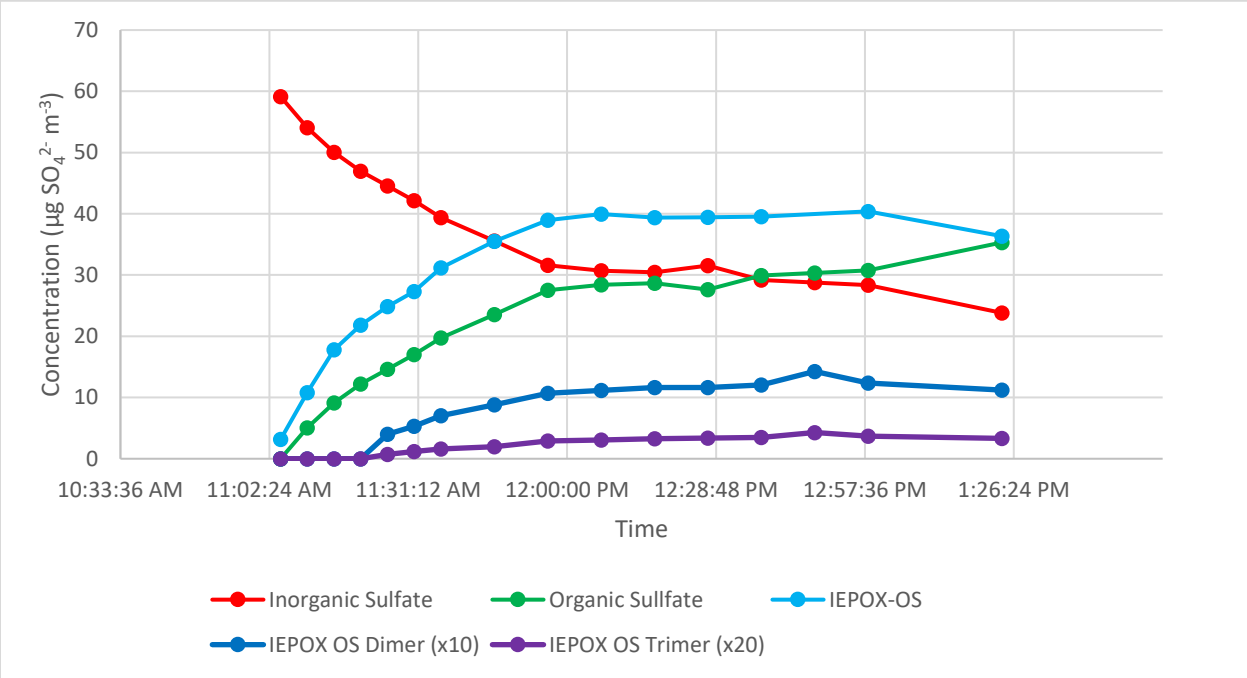


***Figure 13****: Simulated Amazonian Conditions with δ-IEPOX on 3/14/18 (IEPOX:$SO_4^{2-}$ ~42.8)*

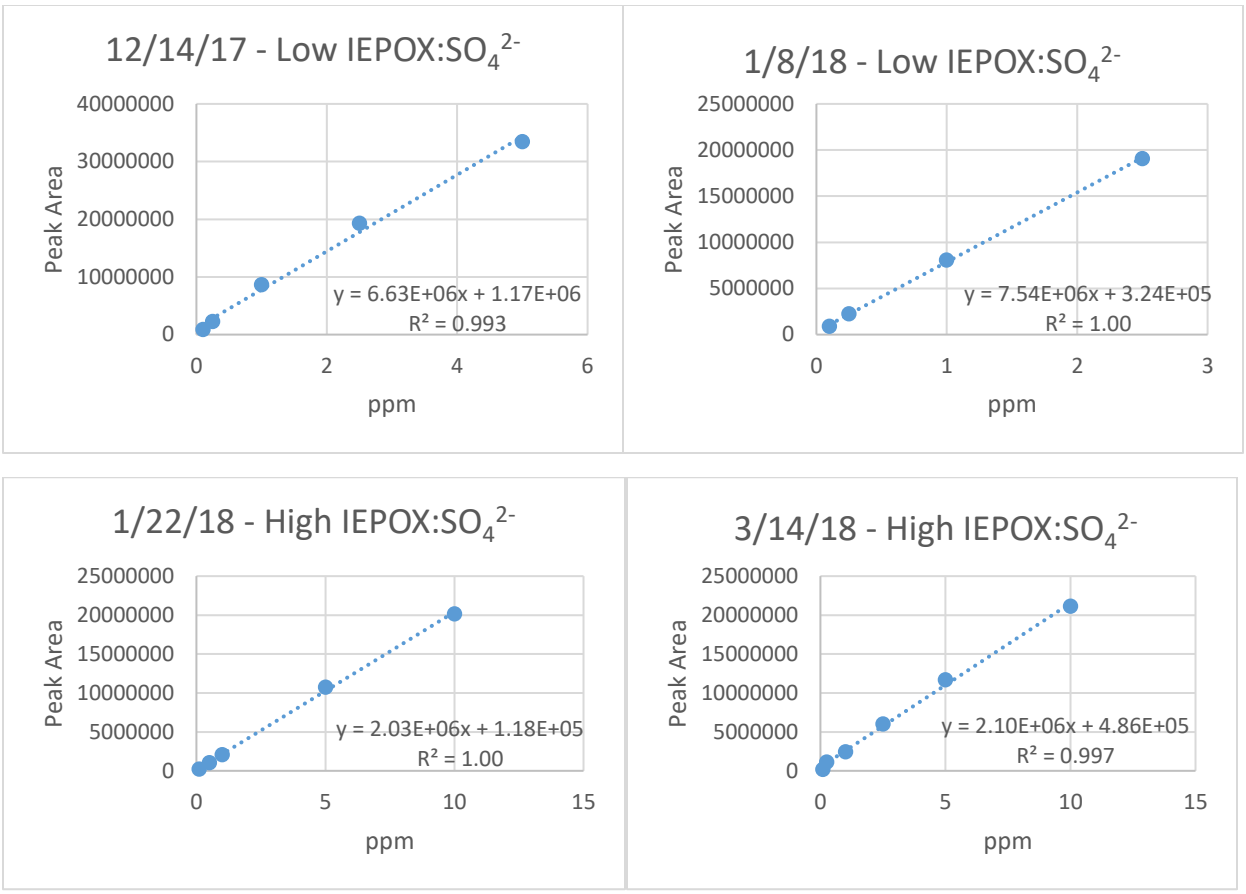


***Figure 14:*** *3-Methyltetrol OS standard curves from UPLC/ESI-HR-QTOFMS analyses conducted in the negative ion mode for the δ-IEPOX experiments. Sample dilution was unnecessary as peak areas all fell within the linear dynamic range.*

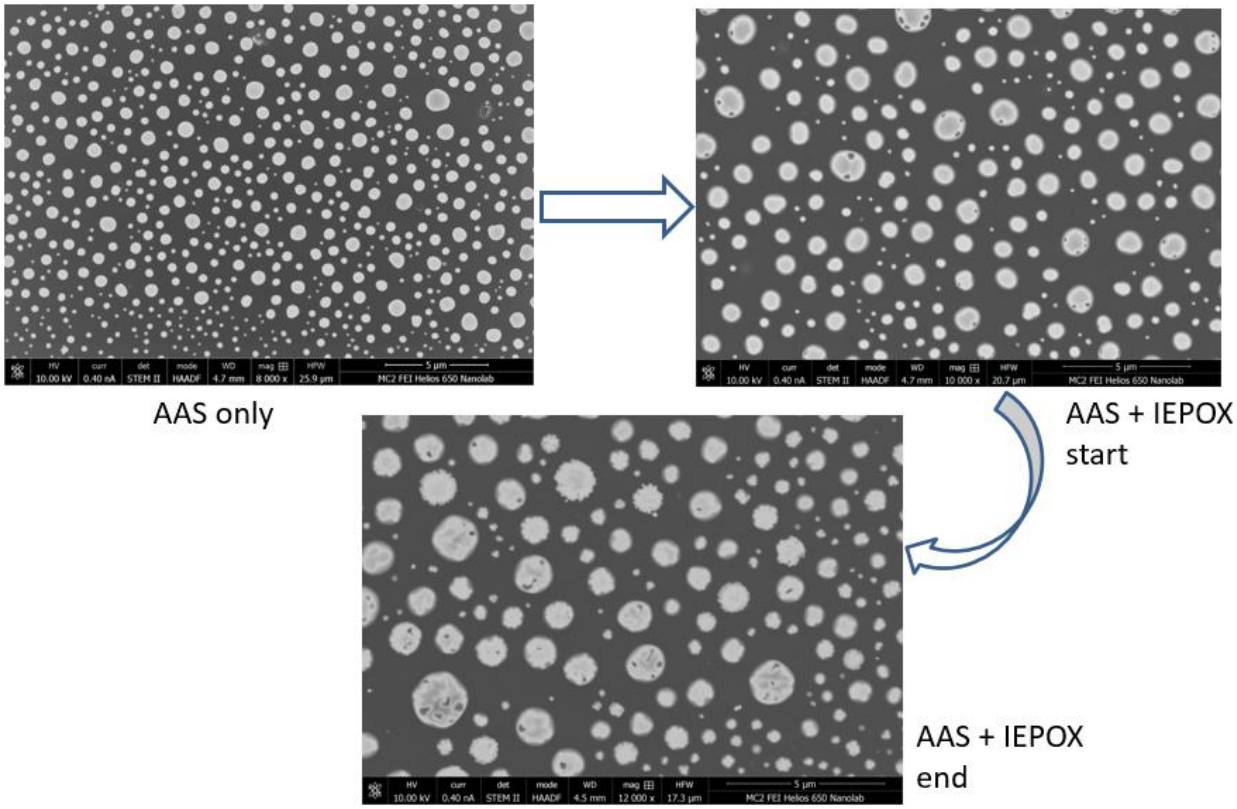


***Figure 15:*** *Microscopy images of δ-IEPOX chamber samples.*

## APPENDIX II: DESCRIPTION OF DATA ANALYISIS AND QUANTIFICATION

### Description of Quantification Using UPLC/ESI-HR-QTOFMS and IC Data

Once offline analysis was completed using UPLC/ESI-HR-QTOFMS, raw peak area data was extracted. In the negative mode, extracted ion chromatograms (EICs) were derived from total ion chromatograms (TICs) at *m/z* ratios corresponding to the weights of the IEPOX-OS monomer, dimer, and trimer (i.e., *m/z* values at 215.0231, 333.0861, and 451.1941, respectively). The peak areas of each species of interest were converted to ppm, and then to a mass concentration, which is reported in Chapter 3. For IC data, chromatographic peaks at retention times corresponding to $SO_4^{2-}$ and $Br^-$ were investigated. The corresponding peak areas were converted to molar concentrations, and the $Br^-$ values were used to calculate the washflow $Br^-$ correction described in Chapter 2. The $SO_4^{2-}$ values were converted to mass concentrations, which correspond to the inorganic sulfate measurements presented in Chapter 3.

## REFERENCES


1. IPCC. (2014). *Summary for Policymakers.* Retrieved from AR5 Synthesis Report: Climate Change 2014: https://www.ipcc.ch/site/assets/uploads/2018/02/AR5_SYR_FINAL_SPM.pdf

2. Charlson, R. J., Schwartz, S. E., Hales, J. M., Cess, R. D., Coakley, J. A., Hansen, J. E., & Hofmann, D. J. (1992). Climate Forcing by Anthropogenic Aerosols. *Science*, *255*(5043), 423 LP-430. https://doi.org/10.1126/science.255.5043.423

3. Dockery, D. W., Pope, C. A., Xu, X., Spengler, J. D., Ware, J. H., Fay, M. E., … Speizer, F. E. (1993). An Association between Air Pollution and Mortality in Six U.S. Cities. *New England Journal of Medicine*. https://doi.org/10.1056/NEJM199312093292401

4. Guenther, A. et al. Estimates of global terrestrial isoprene emissions using MEGAN (Model of Emissions of Gases and Aerosols from Nature). Atmos. Chem. Phys. 6, 3181–3210 (2006).

5. Intergovernmental Panel on Climate Change, Ed., *Climate Change 2013 - The Physical Science Basis: Working Group I Contribution to the Fifth Assessment Report of the Intergovernmental Panel on Climate Change* (Cambridge University Press, Cambridge, 2014; http://ebooks.cambridge.org/ref/id/CBO9781107415324).

6. Laskin, A., Laskin, J., & Nizkorodov, S. A. (2015). Chemistry of Atmospheric Brown Carbon. *Chemical Reviews*. https://doi.org/10.1021/cr5006167

7. Atkinson, R., & Arey, J. (2003). Atmospheric Degradation of Volatile Organic Compounds. *Chemical Reviews*, *103*(12), 4605–4638. https://doi.org/10.1021/cr0206420

8. Jimenez, J. L., Canagaratna, M. R., Donahue, N. M., Prevot, A. S. H., Zhang, Q., Kroll, J. H., … Worsnop, D. R. (2009). Evolution of Organic Aerosols in the Atmosphere. *Science*, *326*(5959), 1525 LP-1529. https://doi.org/10.1126/science.1180353

9. Guenther, A. et al. Estimates of global terrestrial isoprene emissions using MEGAN (Model of Emissions of Gases and Aerosols from Nature). Atmos. Chem. Phys. 6, 3181–3210 (2006).

10. Kiehl, J. T., & Briegleb, B. P. (1993). The Relative Roles of Sulfate Aerosols and Greenhouse Gases in Climate Forcing. *Science*, *260*(5106), 311 LP-314. https://doi.org/10.1126/science.260.5106.311

11. Pope, C. A., & Dockery, D. W. (2006). Health Effects of Fine Particulate Air Pollution: Lines that Connect. *Journal of the Air & Waste Management Association*, *56*(6), 709–742. https://doi.org/10.1080/10473289.2006.10464485

12. Chameides, W. L., Lindsay, R. W., Richardson, J., & Kiang, C. S. (1988). The role of biogenic hydrocarbons in urban photochemical smog: Atlanta as a case study. *Science*. https://doi.org/10.1126/science.3420404

13. Kamens, R. M., Gery, M. W., Jeffries, H. E., Jackson, M., & Cole, E. I. (1982). Ozone–isoprene reactions: Product formation and aerosol potential. *International Journal of Chemical Kinetics*. https://doi.org/10.1002/kin.550140902

14. Pandis, S. N., Paulson, S. E., Seinfeld, J. H., & Flagan, R. C. (1991). Aerosol formation in the photooxidation of isoprene and β-pinene. *Atmospheric Environment Part A, General Topics*. https://doi.org/10.1016/0960-1686(91)90141-S

15. Claeys, M.; Graham, B.; Vas, G.; Wang, W.; Vermeylen, R.; Pashynska, V.; Cafmeyer, J.; Guyon, P.; Andreae, M. O.; Artaxo, P. Formation of secondary organic aerosols through photooxidation of isoprene. Science 2004, 303 (5661), 1173–1176.

16. Kroll, J. H., Ng, N. L., Murphy, S. M., Flagan, R. C., & Seinfeld, J. H. (2006). Secondary organic aerosol formation from isoprene photooxidation. *Environmental Science and Technology*. https://doi.org/10.1021/es0524301

17. Surratt, J. D., Murphy, S. M., Kroll, J. H., Ng, N. L., Hildebrandt, L., Sorooshian, A., … Seinfeld, J. H. (2006). Chemical composition of secondary organic aerosol formed from the photooxidation of isoprene. *Journal of Physical Chemistry A*, *110*(31), 9665–9690. https://doi.org/10.1021/jp061734m

18. Surratt, J. D., Lewandowski, M., Offenberg, J. H., Jaoui, M., Kleindienst, T. E., Edney, E. O., & Seinfeld, J. H. (2007). Effect of acidity on secondary organic aerosol formation from isoprene. *Environmental Science and Technology*. https://doi.org/10.1021/es0704176

19. Surratt, J. D. *et al.* Reactive intermediates revealed in secondary organic aerosol formation from isoprene. *Proc. Natl. Acad. Sci. U. S. A.* **107,** 6640–6645 (2010).

20. Paulot, F., Crounse, J. D., Kjaergaard, H. G., Kürten, A., Clair, J. M. S., Seinfeld, J. H., & Wennberg, P. O. (2009). Unexpected epoxide formation in the gas-phase photooxidation of isoprene. *Science*, *325*(5941), 730–733. https://doi.org/10.1126/science.1172910

21. Lin, Y. H., Zhang, Z., Docherty, K. S., Zhang, H., Budisulistiorini, S. H., Rubitschun, C. L., … Surratt, J. D. (2012). Isoprene epoxydiols as precursors to secondary organic aerosol formation: Acid-catalyzed reactive uptake studies with authentic compounds. *Environmental Science and Technology*. https://doi.org/10.1021/es202554c

22. Lin, Y.-H. *et al.* Epoxide as a precursor to secondary organic aerosol formation from isoprene photooxidation in the presence of nitrogen oxides. *Proc. Natl. Acad. Sci. U. S. A.* **110,** 6718–23 (2013).

23. Zhang, Z. *et al.* Technical Note: Synthesis of isoprene atmospheric oxidation products: isomeric epoxydiols and the rearrangement products *cis*- and *trans*-3-methyl-3,4-dihydroxytetrahydrofuran. *Atmos. Chem. Phys.* **12,** 8529–8535 (2012).

24. Jacobs, M. I., Burke, W. J., & Elrod, M. J. (2014). Kinetics of the reactions of isoprene-derived hydroxynitrates: Gas phase epoxide formation and solution phase hydrolysis. *Atmospheric Chemistry and Physics*. https://doi.org/10.5194/acp-14-8933-2014

25. Bates, K. H., Crounse, J. D., St. Clair, J. M., Bennett, N. B., Nguyen, T. B., Seinfeld, J. H., … Wennberg, P. O. (2014). Gas phase production and loss of isoprene epoxydiols. *Journal of Physical Chemistry A*. https://doi.org/10.1021/jp4107958

26. Nguyen, T. B., Coggon, M. M., Bates, K. H., Zhang, X., Schwantes, R. H., Schilling, K. A., … Seinfeld, J. H. (2014). Organic aerosol formation from the reactive uptake of isoprene epoxydiols (IEPOX) onto non-acidified inorganic seeds. *Atmospheric Chemistry and Physics*. https://doi.org/10.5194/acp-14-3497-2014

27. de Sá, S. S., Palm, B. B., Campuzano-Jost, P., Day, D. A., Newburn, M. K., Hu, W., … Martin, S. T. (2017). Influence of urban pollution on the production of organic particulate matter from isoprene epoxydiols in central Amazonia. *Atmos. Chem. Phys.*, *17*(11), 6611–6629. https://doi.org/10.5194/acp-17-6611-2017

28. Riva, M., Chen, Y., *et al*. (2019). Increasing Importance of Organosulfur Species for 1 Aerosol Properties and Future Air Quality. *Environmental Science & Technology*. Manuscript submitted for publication.

29. Carlton, A. G., De Gouw, J., Jimenez, J. L., Ambrose, J. L., Attwood, A. R., Brown, S., … Zhou, X. (2018). Synthesis of the southeast atmosphere studies: Investigating fundamental atmospheric chemistry questions. *Bulletin of the American Meteorological Society*. https://doi.org/10.1175/BAMS-D-16-0048.1

30. Gaston, C. J., Riedel, T. P., Zhang, Z., Gold, A., Surratt, J. D., & Thornton, J. A. (2014). Reactive uptake of an isoprene-derived epoxydiol to submicron aerosol particles. *Environmental Science and Technology*. https://doi.org/10.1021/es5034266

31. Riedel, T. P., Lin, Y. H., Budisulistiorini, S. H., Gaston, C. J., Thornton, J. A., Zhang, Z., … Surratt, J. D. (2015). Heterogeneous reactions of isoprene-derived epoxides: Reaction probabilities and molar secondary organic aerosol yield estimates. *Environmental Science and Technology Letters*. https://doi.org/10.1021/ez500406f

32. Xu, L., Guo, H., Boyd, C. M., Klein, M., Bougiatioti, A., Cerully, K. M., … Ng, N. L. (2015). Effects of anthropogenic emissions on aerosol formation from isoprene and monoterpenes in the southeastern United States. *Proceedings of the National Academy of Sciences*. https://doi.org/10.1073/pnas.1417609112

33. Riedel, T. P., Lin, Y. H., Zhang, Z., Chu, K., Thornton, J. A., Vizuete, W., … Surratt, J. D. (2016). Constraining condensed-phase formation kinetics of secondary organic aerosol components from isoprene epoxydiols. *Atmospheric Chemistry and Physics*. https://doi.org/10.5194/acp-16-1245-2016

34. Zhang, Y., Chen, Y., Lambe, A. T., Olson, N. E., Lei, Z., Craig, R. L., … Surratt, J. D. (2018). Effect of the Aerosol-Phase State on Secondary Organic Aerosol Formation from the Reactive Uptake of Isoprene-Derived Epoxydiols (IEPOX). *Environmental Science and Technology Letters*. https://doi.org/10.1021/acs.estlett.8b00044

35. Tomaz, S., Cui, T., Chen, Y., Sexton, K. G., Roberts, J. M., Warneke, C., … Turpin, B. J. (2018). Photochemical Cloud Processing of Primary Wildfire Emissions as a Potential Source of Secondary Organic Aerosol. *Environmental Science & Technology*, *52*(19), 11027–11037. https://doi.org/10.1021/acs.est.8b03293

36. Minerath, E. C., & Elrod, M. J. (2009). Assessing the Potential for Diol and Hydroxy Sulfate Ester Formation from the Reaction of Epoxides in Tropospheric Aerosols. *Environmental Science & Technology*, *43*(5), 1386–1392. https://doi.org/10.1021/es8029076

37. Cui, T., Zeng, Z., dos Santos, E. O., Zhang, Z., Chen, Y., Zhang, Y., … Surratt, J. D. (2018). Development of a hydrophilic interaction liquid chromatography (HILIC) method for the chemical characterization of water-soluble isoprene epoxydiol (IEPOX)-derived secondary organic aerosol. *Environmental Science: Processes & Impacts*, *20*(11), 1524–1536. https://doi.org/10.1039/C8EM00308D

38. R. J. Weber, H. Guo, A. G. Russell, A. Nenes, High aerosol acidity despite declining atmospheric sulfate concentrations over the past 15 years. *Nature Geoscience*. **9**, 282–285 (2016).